



HYDROMAGNETIC FREE CONVECTIVE RADIATING FLOW OF CHEMICALLY REACTING FLUID THROUGH POROUS MEDIUM OVER A VERTICAL SURFACE IN THE PRESENCE OF HEAT ABSORPTION

G. Muni Sarala¹ S.V.K. Varma² and N. Chaturvedi^{3*}

¹Research Scholar, Department of Mathematics, S.V.University, Tirupati, A.P.

²Professor, Department of Mathematics, S.V.University, Tirupati.

^{3*} Senior Lecturer, Department of Mathematics, University of Botswana, Gaborone, Botswana.

ABSTRACT

This paper discusses the analysis of first order homogeneous chemical reaction and heat source on MHD flow with heat and mass transfer characteristics of an incompressible, viscous, electrically conducting and Newtonian fluid. An analysis was done over a vertical oscillating porous plate embedded in a porous medium. The fluid considered here is a gray, absorbing/emitting radiation but a non-scattering medium. At time $\bar{t} > 0$, the plate starts oscillating in its own plane with a velocity $u_0 \cos(\omega \bar{t})$. And at the same time, the plate temperature and concentration levels near the plate raised linearly with time \bar{t} . The dimensionless governing equations for momentum, energy and concentration have been solved by using the Laplace transform technique. The velocity, temperature, concentration, skin-friction, the rate of heat transfer and the rate of mass transfer are studied through graphs and tables in terms of different physical parameters entering into the problem.

KEY WORDS

Magnetohydrodynamics, heat and mass transfer, thermal radiation, heat source, chemical reaction, porous medium, vertical plate.

NOMENCLATURE

A	A constant	B_0	External magnetic field
\bar{a}	Absorption coefficient	C_p	Specific heat at constant pressure

\bar{C}	Species concentration	\bar{T}_∞	Fluid temperature in the free stream
\bar{C}_w	Species concentration at the surface	t	Time parameter
\bar{C}_∞	Species concentration in the free stream	u_0	Velocity of the plate
D	Chemical molecular diffusivity	u	Dimensionless velocity
Gm	Mass Grashof number	(\bar{u}, \bar{v})	Velocity components along (\bar{x}, \bar{y}) -directions
Gr	Thermal Grashof number		
g	Acceleration due to gravity		
H	Heat source parameter	Greek symbols	
K	Dimensionless permeability parameter	β	Volumetric coefficient of thermal expansion
\bar{K}	Permeability of the porous medium	$\bar{\beta}$	Volumetric coefficient of concentration expansion
K_r	Dimensionless chemical reaction parameter	κ	Thermal conductivity of the fluid
\bar{K}_r	Chemical reaction parameter	μ	Coefficient of viscosity
M	Magnetic field parameter	ν	Kinematic viscosity
Nu	Nusselt number	ρ	Density of the fluid
Pr	Prandtl number	σ	Electric conductivity
Q_0	Dimensional heat absorption coefficient	$\bar{\sigma}$	Stefan-Boltzmann constant
q_r	Radiative heat flux	τ	Shearing stress
R	Radiative parameter	θ	Dimensionless fluid temperature
Sc	Schmidt number	ϕ	Dimensionless species concentration
Sh	Sherwood number	ω	Frequency of the oscillation
\bar{T}	Temperature	Subscripts	
\bar{T}_w	Fluid temperature at the plate	w	Conditions on the wall
		∞	Free stream conditions

1. INTRODUCTION

In many transport processes in both nature and industrial applications, heat and mass transfer is a consequence of buoyancy effects caused by diffusion of heat and chemical species. Hence, Radiative heat and mass transfer play an important role in manufacturing industries for the design of fins, steel rolling, nuclear power plants, gas turbines and viscous propulsion device for aircraft, missiles, satellites, combustion and furnace design, materials processing, temperature measurements, remote sensing for astronomy and space exploration, energy utilization, cryogenic engineering, food processing, health and military applications, as well as pollution of the environment, formation and dispersion of fog and moisture of agricultural fields. In nature, the existence of pure air or water is impossible, and some foreign mass may be present either naturally or mixed with them. A large number of research works concerning transfer processes with chemical reactions have been reported. In particular, the study of

chemical reaction and heat and mass transfer is of considerable importance in chemical and hydrometallurgical industries. Chambre and Young [3] analyzed a first-order chemical reaction in the neighbourhood of a horizontal plate. A reaction is said to be first-order if the rate of reaction is directly proportional to the concentration itself. In many chemical processes, a chemical reaction occurs between a foreign mass and a fluid in which a plate is moving. Convection in porous media has applications in geothermal energy recovery, oil extraction, thermal energy storage and flow through filtering devices. Convective heat transfer in porous media has received considerable attention in recent years owing to its importance in various technological applications such as fibre and granular insulation, electronic system cooling, cool combustors, and porous material regenerative heat exchangers. In view of these applications, many researchers have studied MHD free convective heat and mass transfer flow in a porous medium. Books by Nield and Bejan[12], Bejan and Kraus[2] and Ingham et al.[7] excellently describe the extent of the research information in this area.

Magnetohydrodynamics has attracted the attention of a large number of scholars due to its diverse applications. In astrophysics and geophysics, it is applied to study the stellar and solar structures, radio propagation through the ionosphere, etc. In engineering we find its applications like in MHD pumps, MHD bearings, etc. The phenomenon of mass transfer is also very common in theory of stellar structure and observable effects are detectable on the solar surface. The study of effects of magnetic field on free convection flow is important in liquid-metals, electrolytes and ionized gases. The thermal physics of hydromagnetic problems with mass transfer is of interest in power engineering and metallurgy. Thermal radiation in fluid dynamics has become a significant branch of the engineering sciences and is an essential aspect of various scenarios in mechanical, aerospace, chemical, environment, solar power, and hazards engineering. If the temperature of surrounding fluid is rather high, radiation effects play an important role and this situation does exist in space technology. In such cases, one has to take into account the combined effect of thermal radiation and mass diffusion. MHD effects on impulsively started vertical infinite plate with variable temperature in the presence of transverse magnetic field were studied by Soundalgekar et al.[16]. The effects transversely applied magnetic field on the flow of an electrically conducting fluid past an impulsively started infinite isothermal vertical plate were also studied by Soundalgekar et al.[17]. The dimensionless governing equations were solved using Laplace transform technique. Kumar and Varma [8] studied the problem of unsteady flow past an infinite vertical permeable plate with constant suction and transverse magnetic field with oscillating plate temperature. Rajput and Kumar [14] considered the radiation effects on MHD flow past an impulsively started vertical plate with variable heat and mass transfer by Laplace transform technique.

In all studies cited above, the flow is driven either by a prescribed surface temperature or by a prescribed surface heat flux. Here, a relatively different driving mechanism for unsteady free convection along a vertical surface is considered where it is assumed that the flow is also set up by Newtonian heating from the surface. Heat transfer characteristics are dependent on the thermal boundary conditions. In general, there are four common heating processes specifying the wall-to-ambient temperature distributions, namely, prescribed wall temperature

distributions(power-law wall temperature distribution along the surface has been usually used); prescribed surface heat flux distributions; conjugate conditions, where heat is supplied through a bounding surface of finite thickness and finite heat capacity. The interface temperature is not known a priori but depends on the intrinsic properties of the system, namely the thermal conductivities of the fluid and solid respectively; Newtonian heating, where the heat transfer rate from the bounding surface with a finite heat capacity is proportional to the local surface temperature and which is usually termed conjugate convective flow. This configuration occurs in many important engineering devices, for example:

- (i) in heat exchangers where the conduction in solid tube wall greatly influenced by the convection in the fluid flowing over it;
- (ii) for conjugate heat transfer around fins where the conduction within the fin and the convection in the fluid surrounding it must be simultaneously analysed in order to obtain vital design information; and
- (iii) in convective flows set up when the bounding surfaces absorb heat by solar radiation.

Therefore, we conclude that the conventional assumption of no interaction of conduction-convection coupled effects is not always realistic and it must be considered when evaluating the conjugate heat transfer processes in many practical engineering applications. Newtonian heating condition has been only recently used in convective heat transfer. Merkin [9] was the first to consider the free convection boundary layer over a vertical flat plate immersed in a viscous fluid.

Chamkha [4] presented an analytical solution for heat and mass transfer by laminar flow of a Newtonian, viscous, electrically conducting fluid and heat generation/absorption. Narahari and Nayan[11] considered free convection flow past an impulsively started infinite vertical plate with Newtonian heating in the presence of thermal radiation and mass diffusion. The effects of mass transfer on flow past an impulsively started infinite vertical plate with Newtonian heating and chemical reaction was analysed by Rajesh[13]. The free convection flow of a viscous incompressible fluid past an infinite vertical oscillating plate with uniform heat flux in the presence of thermal radiation was studied by Chandrakala [5]. Rathod and Asha [15] examined magnetic field effects on two-dimensional viscous incompressible Newtonian fluid with the help of numerical technique. An exact solution to the flow of a viscous incompressible unsteady flow past an infinite vertical oscillating plate with variable temperature and mass diffusion by taking into account of the homogeneous chemical reaction of first-order was investigated by Muthucumaraswamy et al. [10]. Chaudhary et al. [6] investigated the MHD flow past an infinite vertical oscillating plate through porous medium, taking account of the presence of free convection and mass transfer. Ahmed and Kalita[1] studied the MHD radiating flow over an infinite vertical surface bounded by a porous medium in presence of chemical reaction.

The main objective of this paper is to extend the work of reference [1] in the direction to consider the heat source effect. Hence, the present paper, is aimed to study the effects of

transverse magnetic field, thermal radiation, and heat source and first-order chemical reaction on unsteady MHD flow through porous medium over an infinite vertical oscillating plate with variable temperature and mass diffusion. The temperature and concentration of the plate is oscillating with time about a constant non-zero mean value. The dimensionless governing equations involved in the present analysis are solved by using the Laplace transform technique.

2. MATHEMATICAL FORMULATION

Thermal diffusion and radiation effects on unsteady MHD flow of a viscous incompressible fluid past along a vertical oscillating plate with variable temperature and also with variable mass diffusion through porous medium in the presence of transverse applied magnetic field, heat source and chemical reaction of first order are studied. The \bar{x} -axis is taken along the plate in the vertical upward direction and the \bar{y} -axis is taken normal to the plate. Initially it is assumed that the plate and fluid at the same temperature \bar{T}_∞ in the stationary condition with concentration level \bar{C}_∞ at all the points. At time $\bar{t} > 0$, the plate starts oscillating in its own plane with a velocity $u_0 \cos(\omega \bar{t})$. And at the same time, the plate temperature and concentration levels near the plate raised linearly with time \bar{t} . A transverse magnetic field of uniform strength B_0 is assumed to be applied normal to the direction of flow. The viscous dissipation and induced magnetic field are assumed to be negligible. The fluid considered here is gray, absorbing/emitting radiation but a non-scattering medium. Since the plate is assumed to be infinitely long in the \bar{x} -axis direction, all the physical variables are functions of \bar{y} and \bar{t} only. Applying the Boussinesq's approximation, the unsteady flow is governed by the following equations.

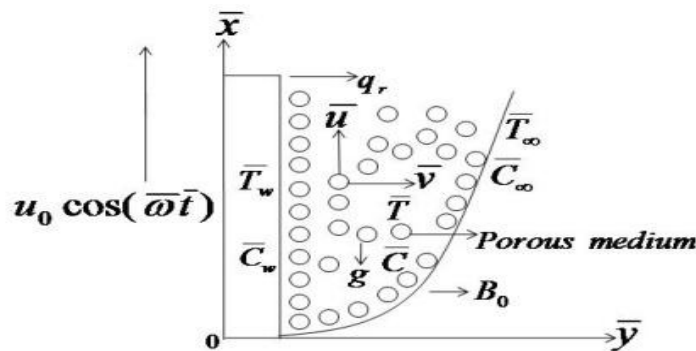


Fig. 1 Physical model and coordinate system

$$\frac{\partial v}{\partial y} = 0$$

(1)

$$\frac{\partial \bar{u}}{\partial \bar{t}} + v \frac{\partial \bar{u}}{\partial y} = g\beta(\bar{T} - \bar{T}_\infty) + g\bar{\beta}(\bar{C} - \bar{C}_\infty) + v \frac{\partial^2 \bar{u}}{\partial \bar{y}^2} - \frac{\sigma B_0^2}{\rho} \bar{u} - \frac{v}{K} \bar{u} \quad (2)$$

$$\rho C_p \frac{\partial \bar{T}}{\partial \bar{t}} + v \frac{\partial \bar{T}}{\partial y} = \kappa \frac{\partial^2 \bar{T}}{\partial \bar{y}^2} - \frac{\partial q_r}{\partial \bar{y}} + Q_0(\bar{T}_\infty - \bar{T})$$

$$(3) \quad \frac{\partial \bar{C}}{\partial \bar{t}} + v \frac{\partial \bar{C}}{\partial y} = D \frac{\partial^2 \bar{C}}{\partial \bar{y}^2} - \bar{K}_r(\bar{C} - \bar{C}_\infty)$$

(4)

The initial and boundary conditions are:

$$\bar{t} \leq 0: \bar{u} = 0, \bar{T} = \bar{T}_\infty, \bar{C} = \bar{C}_\infty \quad \forall \bar{y}$$

$$\bar{t} > 0: \bar{u} = u_0 \cos(\bar{\omega} \bar{t}), \bar{T} = \bar{T}_\infty + (\bar{T}_w - \bar{T}_\infty) A \bar{t}, \bar{C} = \bar{C}_\infty + (\bar{C}_w - \bar{C}_\infty) A \bar{t} \text{ at } \bar{y} = 0$$

(5)

$$\bar{t} > 0: \bar{u} \rightarrow 0, \bar{T} \rightarrow \bar{T}_\infty, \bar{C} \rightarrow \bar{C}_\infty \text{ as } \bar{y} \rightarrow \infty$$

For an optically thin gray gas, the radiative heat flux q_r satisfies the following non-linear differential equation.

$$\frac{\partial q_r}{\partial \bar{y}} = -4\bar{a}\bar{\sigma}(\bar{T}_\infty^4 - \bar{T}^4) \quad (6)$$

where \bar{a} is the absorption coefficient and $\bar{\sigma}$ the Stefan-Boltzmann constant. It is assumed that the temperature differences within the flow are sufficiently small such that \bar{T}^4 may be expressed as a linear function of the fluid temperature \bar{T} using the Taylor's series about the free stream temperature \bar{T}_∞ . After neglecting higher-order terms, gives

$$\bar{T}^4 \cong 4\bar{T}_\infty^3 \bar{T} - 3\bar{T}_\infty^4 \quad (7)$$

Using Eqs.(5) and (6), Eq.(2) becomes

$$\rho C_p \frac{\partial \bar{T}}{\partial \bar{t}} + v \frac{\partial \bar{T}}{\partial y} = \kappa \frac{\partial^2 \bar{T}}{\partial \bar{y}^2} - 16\bar{a}\bar{\sigma}\bar{T}_\infty^3 (\bar{T} - \bar{T}_\infty) + Q_0(\bar{T}_\infty - \bar{T}) \quad (8)$$

The following non-dimensional quantities are introduced:

$$u = \frac{\bar{u}}{u_0}, t = \frac{u_0^2 \bar{t}}{\nu}, y = \frac{u_0 \bar{y}}{\nu}, \theta = \frac{\bar{T} - \bar{T}_\infty}{\bar{T}_w - \bar{T}_\infty}, \phi = \frac{\bar{C} - \bar{C}_\infty}{\bar{C}_w - \bar{C}_\infty}, Sc = \frac{\nu}{D}, Pr = \frac{\rho \nu C_p}{\kappa},$$

$$Gr = \frac{\nu g \beta (\bar{T}_w - \bar{T}_\infty)}{u_0^3}, Gm = \frac{\nu g \bar{\beta} (\bar{C}_w - \bar{C}_\infty)}{u_0^3}, M = \frac{\sigma B_0^2 \nu}{\rho u_0^2}, R = \frac{16\bar{a}\nu^2 \bar{\sigma} \bar{T}_\infty^3}{\kappa u_0^2}, \quad (9)$$

$$\omega = \frac{\bar{\omega} \nu}{u_0^2}, K_r = \frac{\nu \bar{K}_r}{u_0^2}, A = \frac{u_0^2}{\nu}, K = \frac{\bar{K} u_0^2}{\nu}, H = \frac{Q_0 \nu^2}{\kappa u_0^2}$$

In view of Eqs. (8), Eqs. (1), (7), and (3) reduces to the following non-dimensional form, respectively,

$$\frac{\partial u}{\partial t} = \frac{\partial^2 u}{\partial y^2} + Gr\theta + Gm\phi - (M + K^{-1})u$$

(10)

$$\frac{\partial \theta}{\partial t} = \frac{1}{Pr} \frac{\partial^2 \theta}{\partial y^2} - \frac{1}{Pr} (R + H)\theta$$

(11)

$$\frac{\partial \phi}{\partial t} = \frac{1}{Sc} \frac{\partial^2 \phi}{\partial y^2} - K_r \phi$$

(12)

with the following initial and boundary conditions:

$$t \leq 0: u = 0, \theta = 0, \phi = 0 \quad \forall y$$

$$t > 0: u = \cos(\omega t), \theta = t, \phi = t \text{ at } y = 0 \quad (13)$$

$$t > 0: u \rightarrow 0, \theta \rightarrow 0, \phi \rightarrow 0 \text{ as } y \rightarrow \infty$$

where ωt is phase angle

3. SOLUTION OF THE PROBLEM

The appeared physical parameters are defined in the nomenclature. The dimensionless governing equations from (9) to (11), subject to the initial and boundary conditions (12) are solved by the usual Laplace transform technique and the solutions for velocity, temperature and concentration fields are expressed in terms of exponential and complementary error functions.

$$\begin{aligned} u(y,t) = & \frac{1}{4} \exp(i\omega t) \left[\exp(y\sqrt{N+i\omega}) \operatorname{erfc}\left(\frac{y}{2\sqrt{t}} + \sqrt{(N+i\omega)t}\right) + \exp(-y\sqrt{N+i\omega}) \operatorname{erfc}\left(\frac{y}{2\sqrt{t}} - \sqrt{(N+i\omega)t}\right) \right] \\ & + \frac{1}{4} \exp(-i\omega t) \left[\exp(y\sqrt{N-i\omega}) \operatorname{erfc}\left(\frac{y}{2\sqrt{t}} + \sqrt{(N-i\omega)t}\right) + \exp(-y\sqrt{N-i\omega}) \operatorname{erfc}\left(\frac{y}{2\sqrt{t}} - \sqrt{(N-i\omega)t}\right) \right] \\ & - \frac{h}{2} \left[\exp(y\sqrt{N}) \operatorname{erfc}\left(\frac{y}{2\sqrt{t}} + \sqrt{Nt}\right) + \exp(-y\sqrt{N}) \operatorname{erfc}\left(\frac{y}{2\sqrt{t}} - \sqrt{Nt}\right) \right] \\ & + g \left[\left(\frac{t}{2} + \frac{y}{4\sqrt{N}}\right) \exp(y\sqrt{N}) \operatorname{erfc}\left(\frac{y}{2\sqrt{t}} + \sqrt{Nt}\right) + \left(\frac{t}{2} - \frac{y}{4\sqrt{N}}\right) \exp(-y\sqrt{N}) \operatorname{erfc}\left(\frac{y}{2\sqrt{t}} - \sqrt{Nt}\right) \right] \\ & + \frac{l}{2} \exp(-ct) \left[\exp(y\sqrt{N-c}) \operatorname{erfc}\left(\frac{y}{2\sqrt{t}} + \sqrt{(N-c)t}\right) + \exp(-y\sqrt{N-c}) \operatorname{erfc}\left(\frac{y}{2\sqrt{t}} - \sqrt{(N-c)t}\right) \right] \end{aligned}$$

$$\begin{aligned}
& + \frac{m}{2} \exp(-ft) \left[\exp(y\sqrt{N-f}) \operatorname{erfc}\left(\frac{y}{2\sqrt{t}} + \sqrt{(N-f)t}\right) + \exp(-y\sqrt{N-f}) \operatorname{erfc}\left(\frac{y}{2\sqrt{t}} - \sqrt{(N-f)t}\right) \right] \\
& + \frac{l}{2} \left[\exp(y\sqrt{S}) \operatorname{erfc}\left(\frac{y\sqrt{\operatorname{Pr}}}{2\sqrt{t}} + \sqrt{\frac{St}{\operatorname{Pr}}}\right) + \exp(-y\sqrt{S}) \operatorname{erfc}\left(\frac{y\sqrt{\operatorname{Pr}}}{2\sqrt{t}} - \sqrt{\frac{St}{\operatorname{Pr}}}\right) \right] \\
& - r_1 \left[\left(\frac{t}{2} + \frac{y\sqrt{\operatorname{Pr}}}{4\sqrt{S}}\right) \exp(y\sqrt{S}) \operatorname{erfc}\left(\frac{y\sqrt{\operatorname{Pr}}}{2\sqrt{t}} + \sqrt{\frac{St}{\operatorname{Pr}}}\right) + \left(\frac{t}{2} - \frac{y\sqrt{\operatorname{Pr}}}{4\sqrt{S}}\right) \exp(-y\sqrt{S}) \operatorname{erfc}\left(\frac{y\sqrt{\operatorname{Pr}}}{2\sqrt{t}} - \sqrt{\frac{St}{\operatorname{Pr}}}\right) \right] \\
& - \frac{l}{2} \exp(-ct) \left[\exp(y\sqrt{S-c\operatorname{Pr}}) \operatorname{erfc}\left(\frac{y\sqrt{\operatorname{Pr}}}{2\sqrt{t}} + \sqrt{\left(\frac{S}{\operatorname{Pr}} - c\right)t}\right) + \exp(-y\sqrt{S-c\operatorname{Pr}}) \operatorname{erfc}\left(\frac{y\sqrt{\operatorname{Pr}}}{2\sqrt{t}} - \sqrt{\left(\frac{S}{\operatorname{Pr}} - c\right)t}\right) \right] \\
& + \frac{m}{2} \left[\exp(y\sqrt{K_r Sc}) \operatorname{erfc}\left(\frac{y\sqrt{Sc}}{2\sqrt{t}} + \sqrt{K_r t}\right) + \exp(-y\sqrt{K_r Sc}) \operatorname{erfc}\left(\frac{y\sqrt{Sc}}{2\sqrt{t}} - \sqrt{K_r t}\right) \right] \\
& - r_2 \left[\left(\frac{t}{2} + \frac{y\sqrt{Sc}}{4\sqrt{K_r}}\right) \exp(y\sqrt{K_r Sc}) \operatorname{erfc}\left(\frac{y\sqrt{Sc}}{2\sqrt{t}} + \sqrt{K_r t}\right) + \left(\frac{t}{2} - \frac{y\sqrt{Sc}}{4\sqrt{K_r}}\right) \exp(-y\sqrt{K_r Sc}) \operatorname{erfc}\left(\frac{y\sqrt{Sc}}{2\sqrt{t}} - \sqrt{K_r t}\right) \right] \\
& - \frac{m}{2} \exp(-ft) \left[\exp(y\sqrt{(K_r-f)Sc}) \operatorname{erfc}\left(\frac{y\sqrt{Sc}}{2\sqrt{t}} + \sqrt{(K_r-f)t}\right) + \exp(-y\sqrt{(K_r-f)Sc}) \operatorname{erfc}\left(\frac{y\sqrt{Sc}}{2\sqrt{t}} - \sqrt{(K_r-f)t}\right) \right]
\end{aligned}$$

(14)

$$\theta(y,t) = \left(\frac{t}{2} + \frac{y\sqrt{\operatorname{Pr}}}{4\sqrt{S}}\right) \exp(y\sqrt{S}) \operatorname{erfc}\left(\frac{y\sqrt{\operatorname{Pr}}}{2\sqrt{t}} + \sqrt{\frac{St}{\operatorname{Pr}}}\right) + \left(\frac{t}{2} - \frac{y\sqrt{\operatorname{Pr}}}{4\sqrt{S}}\right) \exp(-y\sqrt{S}) \operatorname{erfc}\left(\frac{y\sqrt{\operatorname{Pr}}}{2\sqrt{t}} - \sqrt{\frac{St}{\operatorname{Pr}}}\right)$$

(15)

$$\phi(y,t) = \left(\frac{t}{2} + \frac{y\sqrt{Sc}}{4\sqrt{K_r}}\right) \exp(y\sqrt{K_r Sc}) \operatorname{erfc}\left(\frac{y\sqrt{Sc}}{2\sqrt{t}} + \sqrt{K_r t}\right) + \left(\frac{t}{2} - \frac{y\sqrt{Sc}}{4\sqrt{K_r}}\right) \exp(-y\sqrt{K_r Sc}) \operatorname{erfc}\left(\frac{y\sqrt{Sc}}{2\sqrt{t}} - \sqrt{K_r t}\right)$$

(16)

where

$$\begin{aligned}
S &= R + H, \quad N = M + K^{-1}, \quad b = \frac{Gr}{\operatorname{Pr}-1}, \quad c = \frac{S-N}{\operatorname{Pr}-1}, \quad d = \frac{Gm}{Sc-1}, \quad f = \frac{K_r Sc - N}{Sc-1}, \\
r_1 &= \frac{Gr}{S-N}, \quad r_2 = \frac{Gm}{K_r Sc - N}, \quad l = \frac{Gr(\operatorname{Pr}-1)}{(S-N)^2}, \quad m = \frac{Gm(Sc-1)}{(K_r Sc - N)^2}, \\
g &= \frac{Gr}{S-N} + \frac{Gm}{K_r Sc - N}, \quad h = \frac{Gr(\operatorname{Pr}-1)}{(S-N)^2} + \frac{Gm(Sc-1)}{(K_r Sc - N)^2}
\end{aligned}$$

(17)

SKIN FRICTION:

The boundary layer produces a drag force on the plate due to the viscous stresses which are developed at the wall. The viscous stress at the surface of the plate is given by

$$\begin{aligned}
\tau &= - \left[\frac{\partial u}{\partial y} \right]_{y=0} \\
\tau &= \frac{1}{2} \exp(i\omega t) \left[\sqrt{N+i\omega} \operatorname{erf}(\sqrt{(N+i\omega)t}) + \frac{1}{\sqrt{\pi t}} \exp(-(N+i\omega)t) \right] \\
&+ \frac{1}{2} \exp(-i\omega t) \left[\sqrt{N-i\omega} \operatorname{erf}(\sqrt{(N-i\omega)t}) + \frac{1}{\sqrt{\pi t}} \exp(-(N-i\omega)t) \right] \\
&- h \left[\sqrt{N} \operatorname{erf}(\sqrt{Nt}) + \frac{1}{\sqrt{\pi t}} \exp(-Nt) \right] + g \left[\sqrt{\frac{t}{\pi}} \exp(-Nt) + \left(t\sqrt{N} + \frac{1}{2\sqrt{N}} \right) \operatorname{erf}(\sqrt{Nt}) \right] \\
&+ l \exp(-ct) \left[\sqrt{N-c} \operatorname{erf}(\sqrt{(N-c)t}) + \frac{1}{\sqrt{\pi t}} \exp(-(N-c)t) \right] \\
&+ m \exp(-ft) \left[\sqrt{N-f} \operatorname{erf}(\sqrt{(N-f)t}) + \frac{1}{\sqrt{\pi t}} \exp(-(N-f)t) \right] \\
&+ l \left[\sqrt{\frac{\operatorname{Pr}}{\pi t}} \exp\left(-\frac{St}{\operatorname{Pr}}\right) + \sqrt{S} \operatorname{erf}\left(\sqrt{\frac{St}{\operatorname{Pr}}}\right) \right] - r_1 \left[\sqrt{\frac{t\operatorname{Pr}}{\pi}} \exp\left(-\frac{St}{\operatorname{Pr}}\right) + \left(t\sqrt{S} + \frac{\operatorname{Pr}}{2\sqrt{S}} \right) \operatorname{erf}\left(\sqrt{\frac{St}{\operatorname{Pr}}}\right) \right] \\
&- l \exp(-ct) \left[\sqrt{S-c\operatorname{Pr}} \operatorname{erf}\left(\sqrt{\left(\frac{S}{\operatorname{Pr}}-c\right)t}\right) + \sqrt{\frac{\operatorname{Pr}}{\pi t}} \exp\left(-\left(\frac{S}{\operatorname{Pr}}-c\right)t\right) \right] \\
&+ m \left[\sqrt{\frac{Sc}{\pi t}} \exp(-K_r t) + \sqrt{K_r Sc} \operatorname{erf}(\sqrt{K_r t}) \right] \\
&- r_2 \left[\sqrt{\frac{tSc}{\pi}} \exp(-K_r t) + \sqrt{Sc} \left(t\sqrt{K_r} + \frac{1}{2\sqrt{K_r}} \right) \operatorname{erf}(\sqrt{K_r t}) \right] \\
&- m \exp(-ft) \left[\sqrt{\frac{Sc}{\pi t}} \exp(-(K_r - f)t) + \sqrt{(K_r - f)Sc} \operatorname{erf}(\sqrt{(K_r - f)t}) \right]
\end{aligned} \tag{18}$$

NUSSELT NUMBER:

From temperature field, now we study Nusselt number (rate of change of heat transfer) which is given in non-dimensional form as

$$\begin{aligned}
Nu &= - \left[\frac{\partial \theta}{\partial y} \right]_{y=0} \\
Nu &= \sqrt{\frac{t\operatorname{Pr}}{\pi}} \exp\left(-\frac{St}{\operatorname{Pr}}\right) + \left(t\sqrt{S} + \frac{\operatorname{Pr}}{2\sqrt{S}} \right) \operatorname{erf}\left(\sqrt{\frac{St}{\operatorname{Pr}}}\right)
\end{aligned} \tag{19}$$

SHERWOOD NUMBER:

From concentration field, now we study Sherwood number (rate of change of mass transfer) which is given in non-dimensional form as

$$Sh = - \left[\frac{\partial C}{\partial y} \right]_{y=0}$$
$$Sh = \sqrt{\frac{tSc}{\pi}} \exp(-K_r t) + \sqrt{Sc} \left(t\sqrt{K_r} + \frac{1}{2\sqrt{K_r}} \right) \operatorname{erf}(\sqrt{K_r t}) \quad (20)$$

4. RESULTS & DISCUSSION

In order to get the physical insight in to the problem, numerical computations are carried out to illustrate the effects of different control parameters upon the nature of the flow and transport. The numerical values of the velocity, temperature, concentration, skin-friction, Nusselt number and Sherwood number are computed for different physical parameters $M, Gr, Gm, K, Pr, Sc, K_r, R, H$ and t . A representative set of numerical results is shown graphically in Figs. 2-15 and Tables 1-3. The default values for the control parameters are taken as: $Pr = 0.71$ (air), 7.0 (water), $Sc = 0.22$ (hydrogen), 0.30 (helium), 0.60 (water vapour), 0.78 (ammonia), Phase angle $\omega t = \frac{\pi}{2}$. The other parameters are arbitrarily chosen. In order to check the accuracy of numerical results, the present study (when $H = 0$) is compared with the available theoretical solution of Ahmed and Kalita[1].

Fig. 2 represents the velocity profiles due to the variations in ωt . It is evident from figure that the velocity near the plate exceeds at the plate i.e. the velocity overshoot occurs. Furthermore, the magnitude of the velocity decreases with increasing phase angle (ωt) for air ($Pr = 0.71$). The effect of magnetic field parameter M on the velocity is shown in Fig. 3. The velocity decreases with an increase in the magnetic parameter. It is because that the application of transverse magnetic field will result a resistive type force (Lorentz force) similar to drag force which tends to resist the fluid flow and thus reducing its velocity. Also, the boundary layer thickness decreases with an increase in the magnetic parameter. It is also noticed that the velocity is maximum for air near the plate and decreases with y away from the plate and finally takes an asymptotic value for all values of M .

Fig. 4 illustrates the influences of thermal Grashof number Gr and mass Grashof number Gm on the velocity. It is observed that the velocity increases with increasing values of the thermal Grashof number or mass Grashof number. The thermal Grashof number signifies the relative effect of the thermal buoyancy force to the viscous hydrodynamic force. The mass (solutal) Grashof number defines the ratio of the species buoyancy force to the viscous hydrodynamic force. The flow is accelerated due to the enhancement in buoyancy force corresponding to an increase in the thermal Grashof number i.e., free convection effects. The positive values of

Gr correspond to cooling of the plate by natural convection. Heat is therefore conducted away from vertical plate into the fluid which increases the temperature and thereby enhances the buoyancy force. It is also found that the velocity is maximum for air near the plate and decreases with y away from the plate and finally takes an asymptotic value for all values of Gr and Gm .

The velocity and concentration profiles are plotted for different values of the Schmidt number Sc in Figs. 5 and 6 respectively. The Schmidt number Sc embodies the ratio of the momentum diffusivity to the mass (species) diffusivity. It physically relates the relative thickness of the hydrodynamic boundary layer and mass transfer (concentration) boundary layer. As the Schmidt number increases the concentration decreases. This causes the concentration buoyancy effects to decrease yielding a reduction in the fluid velocity. The reductions in the velocity and concentration profiles are accompanied by simultaneous reductions in the velocity and concentration boundary layers, which is evident from Figs. 5 and 6.

Fig. 7 illustrates the temperature profiles for different values of Prandtl number Pr . From this figure, it is observed that an increase in the Prandtl number results in a decrease of the thermal boundary layer thickness and in general, lower average temperature within the boundary layer. This is due to the fact that thermal conductivity of fluid decreases with increasing Pr , resulting a decrease in the thermal boundary layer thickness.

The effects of radiation parameter R and the heat source parameter H on temperature of the flow field are shown in Fig. 8. It is seen that as radiation parameter R or heat source parameter H increases the temperature of the flow field decreases at all points in flow region.

The influence of chemical reaction parameter K_r on velocity and concentration profiles is presented in Figs. 9 and 10. As expected, the presence of the chemical reaction significantly affects the concentration profiles as well as the velocity profiles. Here, studied case is for destructive chemical reaction ($K_r > 0$). We note from Fig. 9 that there is decrease in velocity profiles with increase in K_r , and presence of the peak indicates that the maximum value of the velocity occurs in the body of the fluid near the surface. Also it is observed from Fig. 10 that increasing value of the K_r , decreases the concentration of species in the boundary layer, this is due to the fact that destructive chemical reduces the solutal boundary layer thickness and increases the mass transfer.

The velocity profiles are shown in Fig. 11 for different values of the permeability parameter K . It is found that the velocity increases with increasing values of K . This is due to the fact that increasing values of K reduces the drag force which assists the fluid considerably to move fast. Also it is noticed that the magnitude of velocity for air is higher than that of water.

The skin-friction is studied in Figs. 12 and 13 against time t . It is noticed that as Gr or Gm or K increases, the skin-friction decreases in Fig. 12, where as in Fig. 13 the skin-friction

increases with increasing R or H or K_r . Also, it is observed that the skin-friction decreases with increasing time.

Fig. 14 illustrates the variation of Nusselt number against time t . From this figure it is observed that Nusselt number increases with increasing R or H for water and the reverse effect is observed with the same values of R and H for air. Also, it is found that the Nusselt number increases with increasing values of Pr and t .

Finally, from Fig.15 it is seen that as Sc or K_r increases, the Sherwood number increases.

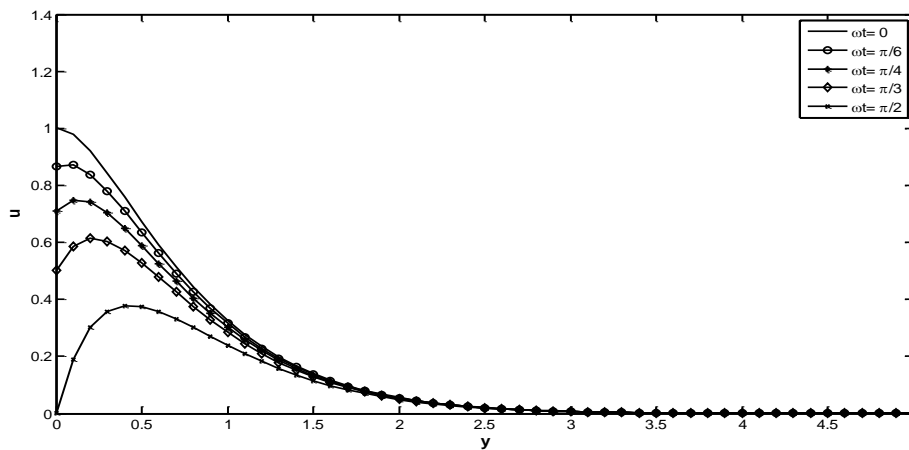


Fig. 2: Velocity profiles for different ωt with $Pr = 0.71, Sc = 0.78, M = 2, K = 0.5,$
 $R = 10, H = 4, Gr = 5, Gm = 5, K_r = 3$

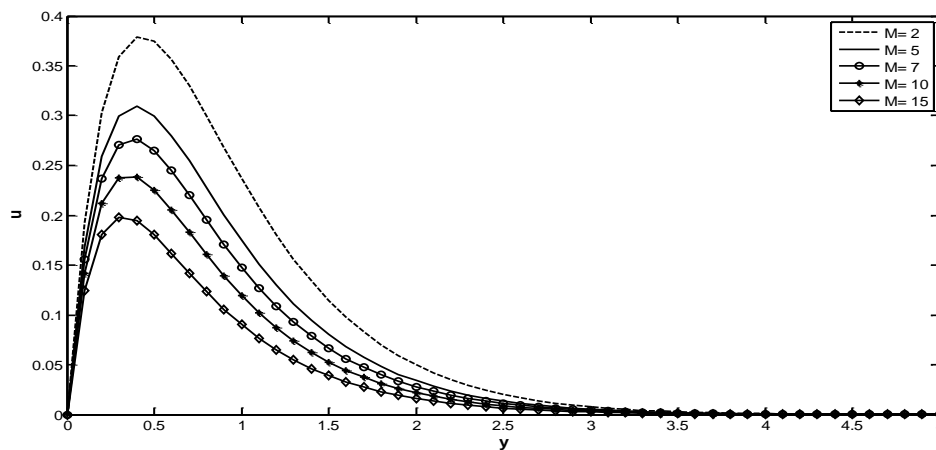


Fig. 3: Velocity profiles for different M with $Pr = 0.71, Sc = 0.78, K = 0.5,$
 $R = 1, H = 4, Gr = 5, Gm = 5, K_r = 1, \omega t = \frac{\pi}{4}$

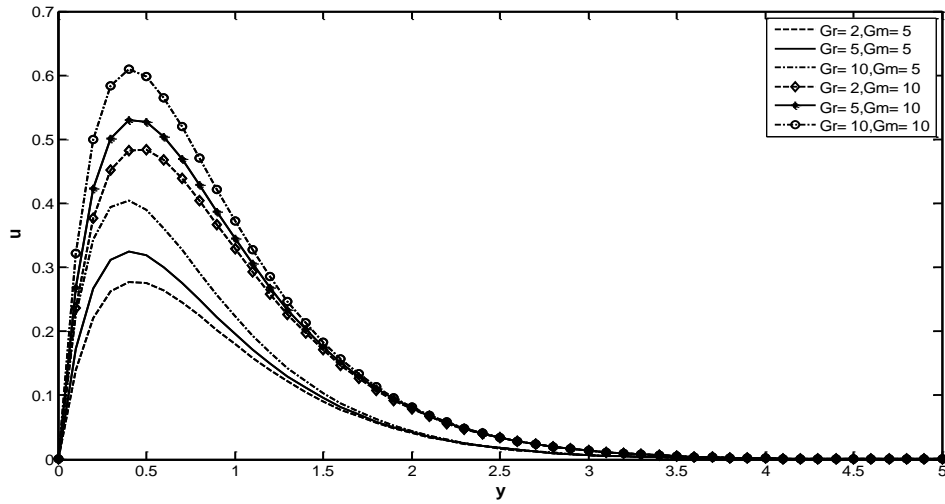


Fig. 4: Velocity profiles for different Gr and Gm with $Pr = 0.71, Sc = 0.78, M = 5,$
 $K = 0.5, R = 10, H = 4, K_r = 1, \omega t = \frac{\pi}{4}$

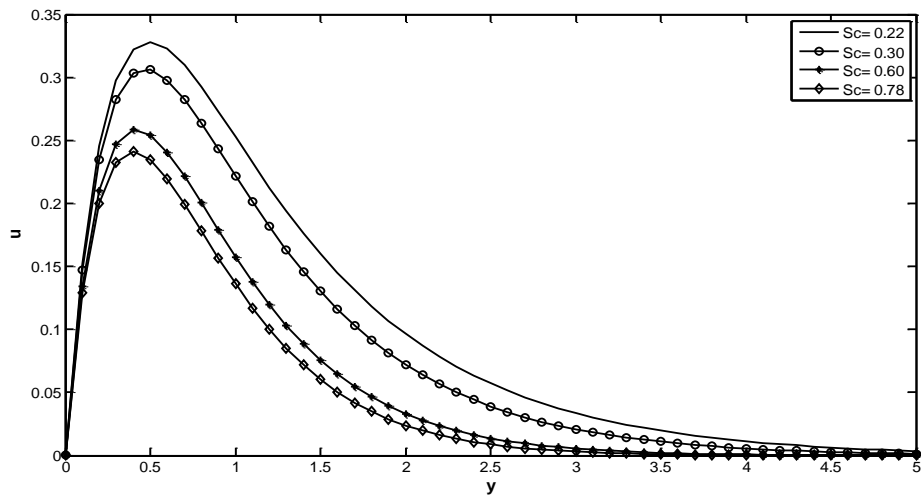


Fig. 5: Velocity profiles for different Sc with $Pr = 0.71, M = 5, K = 0.5, R = 10,$
 $H = 4, Gr = 2, Gm = 5, K_r = 3, \omega t = \frac{\pi}{4}$

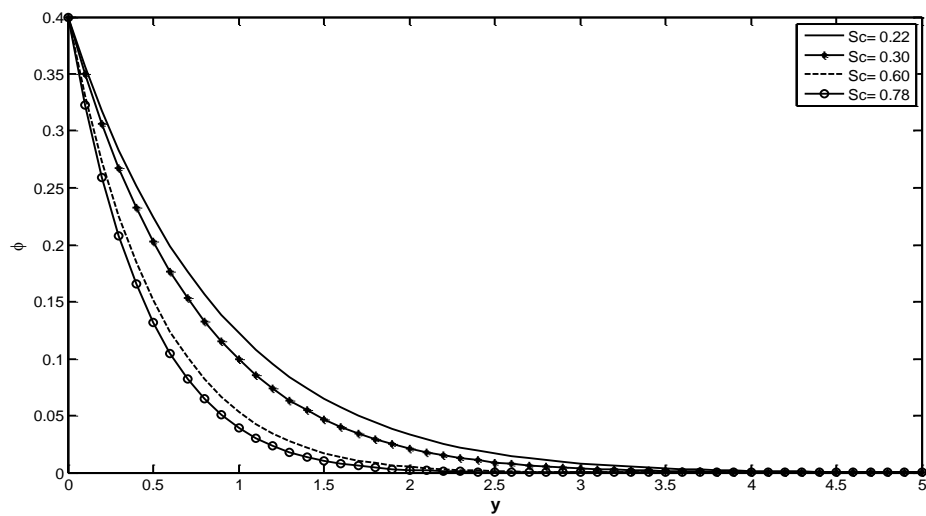


Fig. 6: Concentration profiles for different Sc with $t = 0.4, K_r = 3$

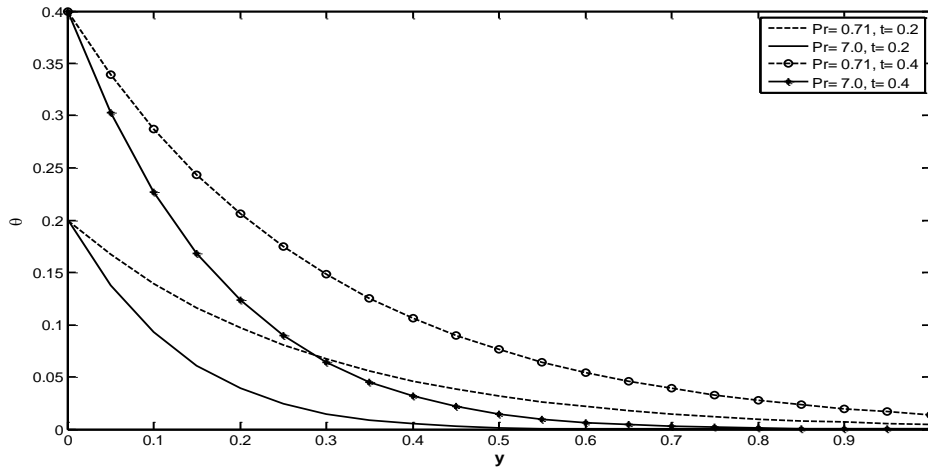


Fig. 7: Temperature profiles for different Pr and t with $R = 5, H = 4$

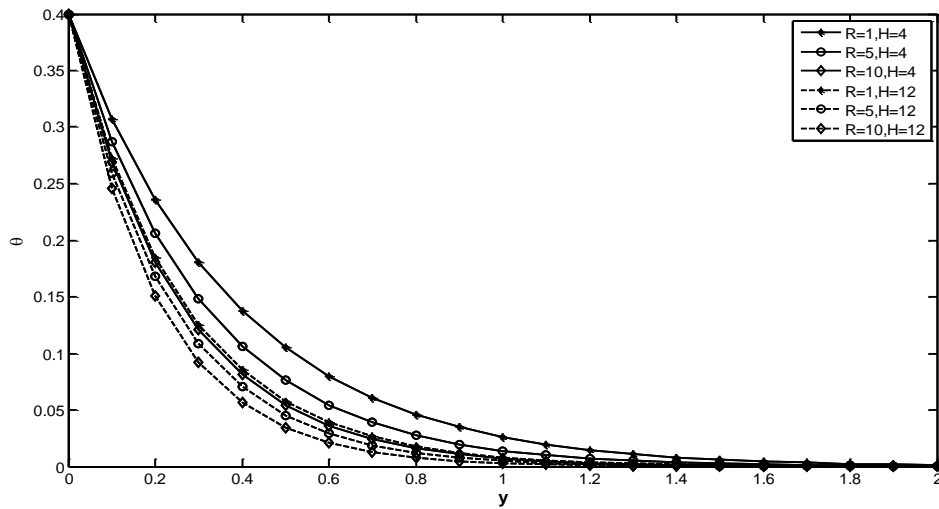


Fig. 8: Temperature profiles for different R and H with $t = 0.4, Pr = 0.71$

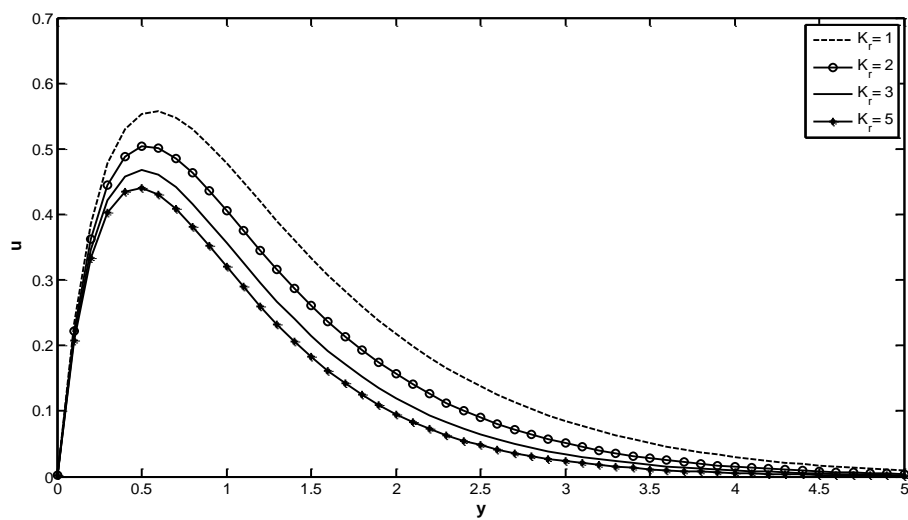


Fig. 9: Velocity profiles for different K_r , with $Pr = 0.71, Sc = 0.78, M = 2, K = 0.5,$

$$R = 10, H = 4, Gr = 5, Gm = 5, \omega t = \frac{\pi}{4}$$

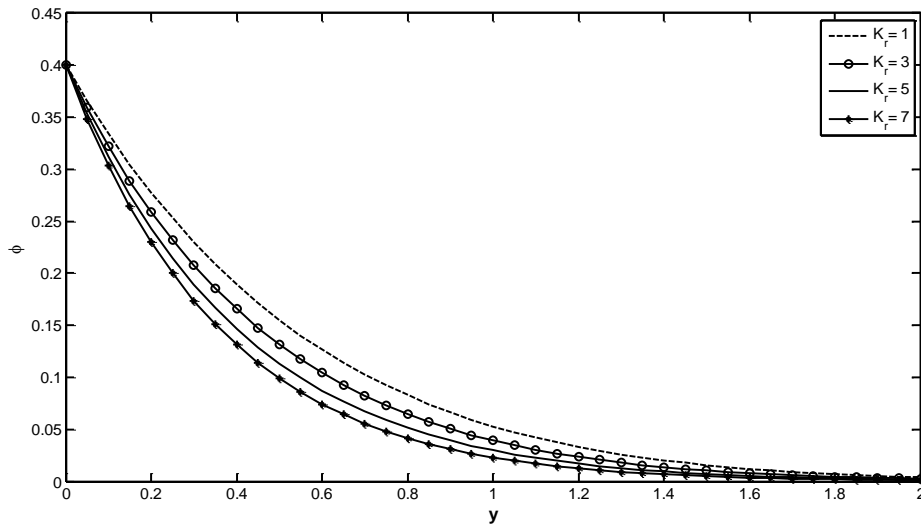


Fig.10: Concentration profiles for different K_r , with $t = 0.4, Sc = 0.78$

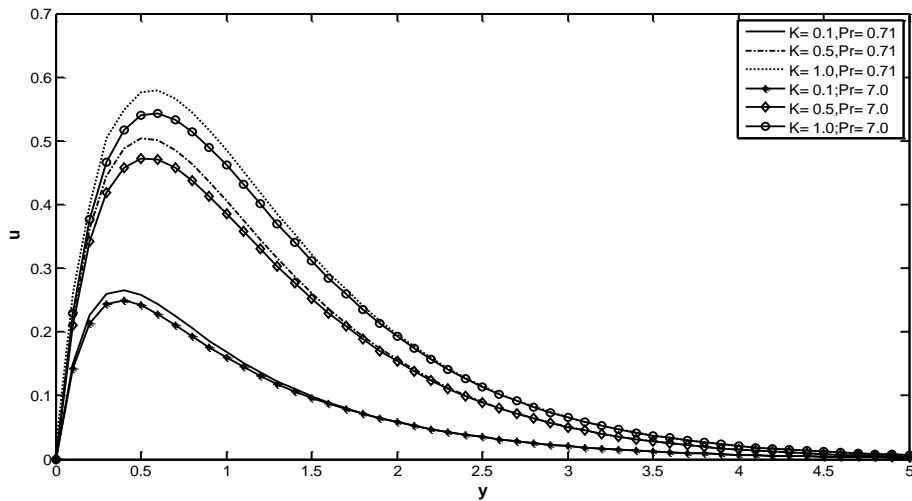


Fig. 11: Velocity profiles for different K and Pr with $Sc = 0.22, M = 2, K_r = 3,$

$$R = 10, H = 4, Gr = 5, Gm = 5, \omega t = \frac{\pi}{4}$$

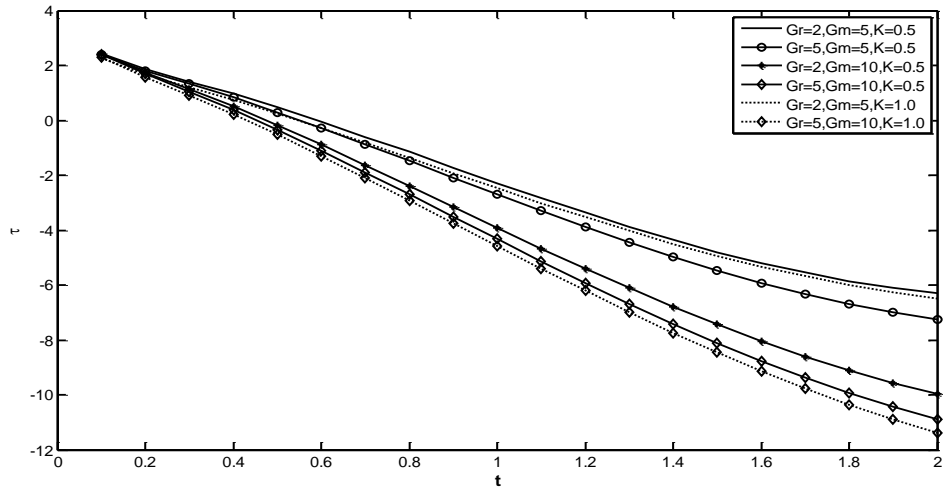


Fig 12: Skin friction for different Gr , Gm and K with $Pr = 7.0, Sc = 0.22, M = 2,$
 $R = 10, H = 4, K_r = 1, \omega t = \frac{\pi}{4}$

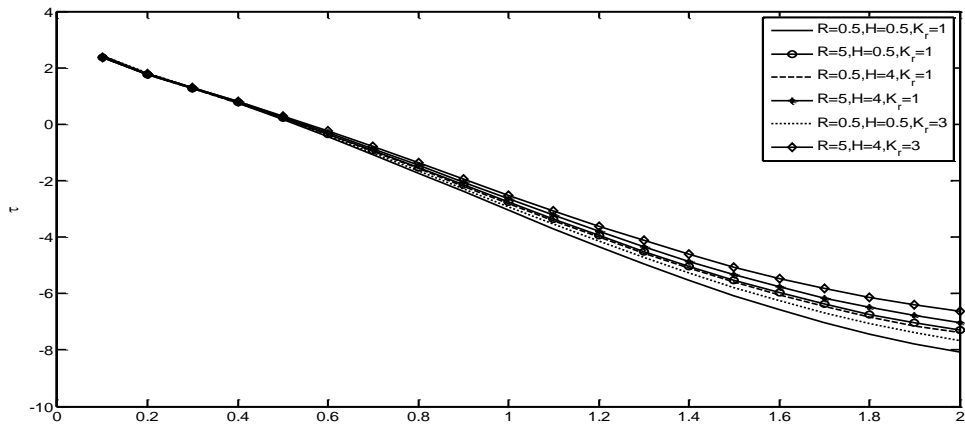


Fig 13: Skin friction for different R , H and K_r with $Pr = 0.71, Sc = 0.78, M = 2,$
 $K = 0.5, Gr = 5, Gm = 5, \omega t = \frac{\pi}{4}$

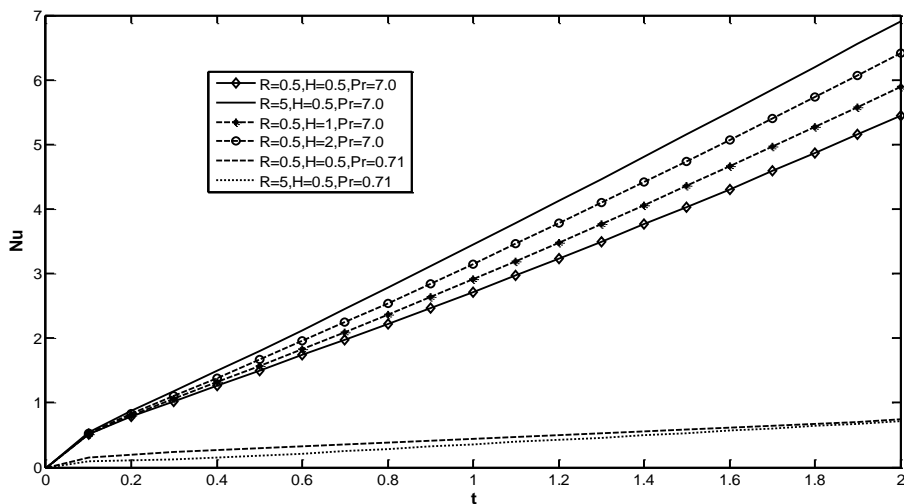


Fig14: Nusselt number for different R and H

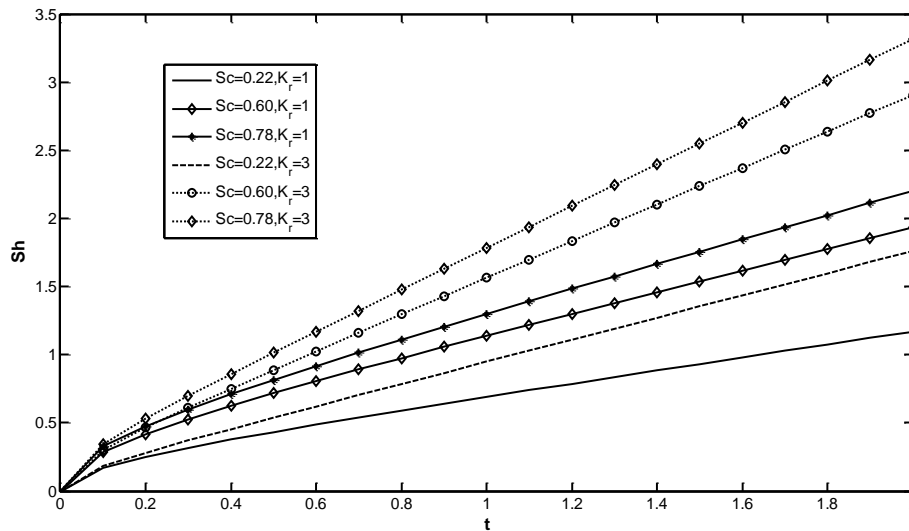


Fig 15: Sherwood number for different Sc and K_r

The effects of various governing parameters on the skin-friction coefficient, Nusselt number and Sherwood number are shown in tables 1, 2 and 3. In all these tables, it is noted that the comparison of each parameter is made with first row in the corresponding table. From table 1, it is observed that as M or R or H or Sc or K_r or Pr increases the skin-friction coefficient increases whereas the skin-friction coefficient decreases as Gr or Gm or K and ωt increases. Table 2 shows that the Nusselt number decreases with increasing R or H for air and the Nusselt number increases with the same values of R and H for water. Also, it is found that the Nusselt number increases with increasing values of Pr and t . Finally, from table 3, it is seen that as Sc or K_r or t increases, the Sherwood number increases.

ωt	Pr	M	Gr	Gm	R	H	Sc	K_r	K	τ
$\frac{\pi}{4}$	0.71	2	5	5	5	1	0.22	1	0.5	1.0834
$\frac{\pi}{4}$	0.71	5	5	5	5	1	0.22	1	0.5	1.7095
$\frac{\pi}{4}$	0.71	2	10	5	5	1	0.22	1	0.5	0.7268
$\frac{\pi}{4}$	0.71	2	5	10	5	1	0.22	1	0.5	0.6262
$\frac{\pi}{4}$	0.71	2	5	5	10	1	0.22	1	0.5	1.1239
$\frac{\pi}{4}$	0.71	2	5	5	5	4	0.22	1	0.5	1.1097
$\frac{\pi}{4}$	0.71	2	5	5	5	1	0.78	1	0.5	1.1602
$\frac{\pi}{4}$	0.71	2	5	5	5	1	0.22	3	0.5	1.1058
$\frac{\pi}{4}$	0.71	2	5	5	5	1	0.22	1	1.0	0.8588
$\frac{\pi}{4}$	7.0	2	5	5	5	1	0.22	1	0.5	1.2094
$\frac{\pi}{2}$	0.71	2	5	5	5	1	0.22	1	0.5	0.6902

Table 1: Numerical values of the skin-friction coefficient (τ)

t	Pr	R	H	Nu
0.4	0.71	5	1	0.1509
0.4	0.71	10	1	0.1426
0.4	0.71	5	4	0.1437
0.4	0.71	10	4	0.1421
0.8	0.71	5	1	0.2844
0.8	0.71	10	4	0.2840
0.4	7.0	5	1	1.4994
0.4	7.0	10	1	1.5365
0.4	7.0	5	4	1.5298
0.4	7.0	10	4	1.5359
0.8	7.0	5	4	2.8531
0.8	7.0	10	1	2.8639

Table 2: Numerical values of Nusselt number (Nu)

t	Sc	C_r	Sh
0.4	0.22	1	0.3777
0.4	0.22	3	0.4549
0.4	0.60	1	0.6237
0.4	0.60	3	0.7513
0.4	0.78	1	0.7111
0.4	0.78	3	0.8566
0.8	0.22	1	0.5906
0.8	0.78	1	1.1120

Table 3: Numerical values of Sherwood number (Sh)

5. CONCLUSIONS

We analyse the effects of chemical reaction, thermal radiation and heat source on unsteady MHD flow of a viscous incompressible fluid past along an infinite vertical oscillating porous plate embedded in a porous medium. The equations of momentum, energy and diffusion which govern the flow field are solved by the usual Laplace transform technique. The results illustrate the flow characteristics for the velocity, temperature, concentration, skin-friction, Nusselt number and Sherwood number.

The conclusions of the study are summarized as follows:

- The velocity decreases with an increase in the phase angle (ωt) for air.
- The velocity decreases with an increase in the magnetic parameter.
- The velocity increased with increased in either of the thermal Grashof number or the mass Grashof number.
- The velocity as well as concentration decreased as the Schmidt number increased.
- An increase in the Prandtl number caused a decrease in the temperature.
- Temperature decreases with an increase in the radiation parameter or heat source parameter.
- The velocity as well as concentration decreases with an increase in the chemical reaction parameter.
- The velocity increases with an increase in the permeability of the porous medium for both air and water.
- The skin-friction decreases as Gr or Gm or K increases, where as the skin-friction increases with increasing R , H and K_r .
- The rate of heat transfer increases due to increase in the radiation parameter or heat source parameter.
- As Schmidt number or chemical reaction parameter increases, the rate of mass transfer increases.

REFERENCES

- [1] Ahmed, S. and Kalita, K., MHD radiating flow over an infinite vertical surface bounded by a porous medium in presence of chemical reaction, Journal of Applied Fluid Mechanics, Vol.6, No.4, pp.597-607, 2013.
- [2] Bejan, A. and Kraus, A.D., Heat Transfer Handbook, Wiley, New York, 2003.
- [3] Chambre, P.L. and Young, J.D., On the diffusion of a chemically reactive species in a laminar boundary layer flow, Phys. Fluids, Vol.1, pp.48-54, 1958.
- [4] Chamkha, A.J., MHD Flow of uniformly stretched vertical permeable surface in the presence of heat generation/absorption and a chemical reaction, Int. Comm. Heat Mass Transfer, Vol.30, pp.413-422, 2003.
- [5] Chandrakala, P., Radiation effects on flow past an impulsively started vertical oscillating plate with uniform heat flux, International Journal of Dynamics of fluids, Vol.6, No.2, pp.209-215, 2010.
- [6] Chaudhary, R.C. and Arpita Jain, Combined heat and mass transfer effects on MHD free convection flow past an oscillating plate embedded in porous medium, Rom. Journ. Phys., Vol.52, Nos.5-7, pp. 505-524, Bucharest, 2007.
- [7] Ingham, D.B., Bejan, A., Mamut, E. and Pop I., Emerging Technologies and Techniques in Porous Media, Kluwer, Dordrecht, 2004.
- [8] Kumar, A.G.V. and Varma, S.V.K., Thermal radiation and mass transfer effects on MHD flow past an impulsively started vertical plate with variable temperature effects variable mass diffusion, Int. Journal of Engineering, Vol.3, pp.493-499, 2011.

- [9] Merkin, J.H., Natural convection boundary-layer flow on a vertical surface with Newtonian heating, *Int. J. Heat fluid flow*, Vol.15 No.5, pp.392-398, 1994.
- [10] Muthucumaraswamy, R., Meenakshisundaram, S., Theoretical study of chemical reaction effects on vertical oscillating plate with variable temperature, *Theoret. Appl. Mech.*, Vol.33, No.3, pp.245-257, Belgrade, 2006.
- [11] Narahari, M. and Nayan, M.Y., Free convection flow an impulsively started infinite vertical plate with Newtonian heating in the presence of thermal radiation and mass diffusion, *Turkish J.Eng. Env. Sci*, Vol.35, pp.187-198, 2011.
- [12] Nield, D.A. and Bejan, A., *Convection in Porous Media*, 2nd edn. Springer, New York, 1999.
- [13] Rajesh, V., Effects of mass transfer on flow past an impulsively started infinite vertical plate with Newtonian heating and chemical reaction, *Journal of Engineering Physics and Thermophysics*, Vol.85, No.1, pp.221-228, 2012.
- [14] Rajput, U.S. and Kumar, S., Radiation effects on MHD flow past an impulsively started vertical plate with variable heat and mass transfer, *Int. J. of Appl. Math. and Mech.*, Vol.8 No.1, pp.66-85, 2012.
- [15] Rathod, V.P., and Asha, S.K., Magnetic field effects on two-dimensional viscous incompressible Newtonian fluid, *Advances in Applied Science Research*, Vol.2, No.4, pp.102-109, 2011.
- [16] Soundalgekar, V.M., Gupta, S.M. and Birajdar, N.S., Effects of mass transfer and free convection currents on MHD Stokes problem for a vertical plate, *Nuclear Engg. Des.*, Vol.53, pp.339-346, 1979.
- [17] Soundalgekar, V.M., Patil, M.R. and Jahagirdar M.D., MHD stokes problem for a vertical plate with variable temperature, *Nuclear Engg. Des.*, Vol.64, pp.39-42, 1981.